A unique {332}<113> twin to α" martensite transition during twin propagation in a Ti-12wt.% Mo alloy with micro-segregation

Xin Ji[a,*,1], Satoshi Emura[a], Koichi Tsuchiya[a,b,] *

[a]Research Center for Structural Materials, National Institute for Materials Science, 1-2-1 Sengen, Tsukuba, Ibaraki 305-0047, Japan

[b]Graduate School of Pure and Applied Sciences, University of Tsukuba, 1-1-1 Tennodai, Tsukuba, Ibaraki 305-8577, Japan

*Corresponding authors: jixin0814@gmail.com (Xin Ji), TSUCHIYA.Koichi@nims.go.jp (Koichi Tsuchiya)

[1]Present address: Technical Research Center, Nippon Yakin Kogyo Co., Ltd., Kawasaki, Kanagawa 210-8558, Japan

Abstract

In this study, the propagation behavior of {332}<113>$_\beta$ twins was investigated in a Ti-12Mo (wt.%) alloy with micro-segregation bands (Mo content ranging from 10 to 13 wt.%). A unique transition from {332}<113>$_\beta$ twins to α"-martensite was observed when those twins propagated across the Mo-lean bands inside the grain. A deflection angle of ~18 º was found between the twin boundary and the α"-martensite plate. This transition was more frequently found at relatively higher stresses. Thermodynamic analysis revealed that the Mo content together with the applied stress govern the required mechanical work for triggering α" martensitic phase transformation. The stress-induced α" martensitic phase transformation was easier to trigger in the Mo-lean bands, with a spontaneous interruption of the {332}<113>$_\beta$ twin propagation. The present chemically segregated microstructure provides a novel approach to comprehensively characterize the variable deformation modes in metastable β titanium alloys.

Keywords: Ti-12Mo, twin propagation, α"-martensite, Mo content, β phase stability

In β-Ti alloys, several deformation modes including stress-induced martensitic (SIM) transformation (bcc-β → orthorhombic-α"), {332}<113>$_\beta$ twinning and dislocation slip, have been frequently reported, depending on the β phase stability of the alloy [1–5]. Molybdenum equivalency ($[Mo]_{eq}$), as a function of the alloying element contents (Mo, Al, V, Fe, etc.) $[Mo]_{eq}$= [Mo] + 2.9 [Fe] + 0.67 [V] + 0.44 [W] + 0.22 [Ta] + 1.6 [Cr] – [Al], in wt.% is commonly used to quantify the β phase stability [6]. Based on a large number of experimental results, it has been empirically suggested that SIM α" is the dominant deformation mechanism in β-Ti alloys with 7.4~12 wt.% $[Mo]_{eq}$ [3,7-8], whereas {332}<113>$_\beta$ twinning takes over at a $[Mo]_{eq}$ range of 10~18 wt.% $[Mo]_{eq}$ [9-11]. In highly stable β-Ti alloys with $[Mo]_{eq}$ > 20 wt.% [12], dislocation slip becomes the major deformation mode. In particular, the coexistence of different deformation modes has been suggested to improve the mechanical performances of β-Ti alloys [3,13]. For instance, Sun *et al*. [3,14] reported a superior combination of strength and work-hardening in a Ti-12Mo (wt.%) alloy, due to the simultaneous occurrence of SIM α", {332}<113>$_\beta$ twins and dislocation slip.

{332}<113>$_\beta$ twinning is known as a unique twinning mode in metastable β-Ti alloys [15]. Several mechanisms have been proposed for the nucleation of {332}<113>$_\beta$ twins, such as shear and shuffle [16,17], partial dislocation [18] and α" martensite-assisted [19] mechanisms. In contrast, relatively less attention has been paid to the propagation behavior of {332}<113>$_\beta$ twins, which also plays a critical role in affecting the work hardening behavior and uniform elongation of the material [20]. Recently, a novel approach of developing chemically heterogeneous microstructure in β-Ti alloys enabled a comprehensive investigation of the solute effects on phase transformation [21,22], precipitation kinetics [23] and twin propagation behaviors [24,25]. For example, in a multilayered Ti-10Mo-*x*Fe (x = 1~3, wt.%) alloy processed by hot rolling, the propagation of {332}<113>$_\beta$ twin was interrupted at the boundary of highly stabilized β matrix ($[Mo]_{eq}$ > 15.8 wt.%) with a higher Fe content. This was explained by a higher stress required for twin propagation in high Fe concentration regions [24,25]. Similarly, Mo-segregation bands were also reported in a Ti-12wt.% Mo model alloy processed by conventional hot rolling method. This begs the question of whether and how the propagation behavior of {332}<113>$_\beta$ twins will be affected at the chemically heterogeneous interfaces, and if so, what the underlying mechanism for this effect.

A Ti-12Mo (wt.%) ingot was prepared by cold crucible levitation melting. The chemically heterogeneous microstructure was produced by hot forging at 1273 K, and then hot rolling at 923 K into a 14.3 mm square bar followed by air-cooling. The material was solution-treated at 1073 K for 1 hour in the single β phase region followed by water quenching. Both the forging and rolling temperatures were deliberately chosen to be lower than those required (forging temperature: 1473 K and rolling temperature: 1423 K, based on our previous study [26]) to fully homogenize Mo element. In addition, no homogenization treatment was carried out in this study. Tensile specimens with a gauge geometry of 18 mm (length) × 4 mm (width) × 2 mm

(thickness) were machined with the tensile axis (TA) parallel to rolling direction (RD). Interrupted tensile tests up to a strain (ε) of 4.5% were performed in an INSTRON 5581 testing machine with an initial strain rate of 2.8×10^{-4} s^{-1} at ambient temperature. Microstructural characterization was performed on the same region of the sample at each interrupted strain by backscattered electron (BSE) imaging and electron backscatter diffraction (EBSD). BSE imaging was carried out on a Zeiss Σ scanning electron microscope (SEM). EBSD measurements were conducted on a JEOL JSM-7001F field emission gun-SEM equipped with a TSL OIM EBSD system operated at 20 kV and the step size of 0.1μm. Distribution of Mo was measured by JEOL JXA-8900F electron probe micro-analyzer (EPMA).

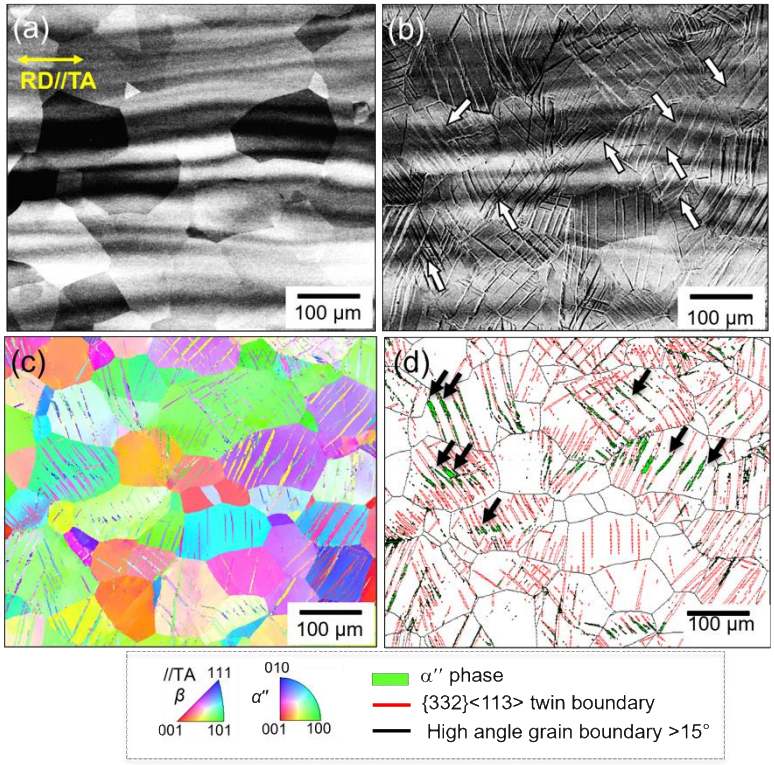

Fig. 1 (a) BSE image of the microstructure prior to deformation. The tensile axis (TA) is parallel to the rolling direction (RD), as shown in the image. (b) BSE image of identical area as (a) after a strain of 4.5%. (c) Inverse pole figure (IPF) map of the deformed microstructure. (d) Boundary map (red line: {332}<113> twin boundary, black line: high angle grain boundary with a misorientation angle θ >15°) of the deformed microstructure, in which α" phase was indicated by green color.

A BSE image of the chemically heterogenous microstructure before tensile deformation is shown in **Fig. 1(a)**. The alternating dark and bright bands aligned parallel to RD correspond the Mo-lean (~ 10 wt.% Mo) and Mo-rich (~ 13 wt.% Mo) regions, respectively [27]. These micro-segregation bands are about 20~40 μm in thickness. A BSE image of the same area after tensile deformation (by a strain of 4.5%) is shown in **Fig. 1(b)**, in which numerous plate-like deformation products can be observed. It is interesting to note that

some of the plates (indicated by the white arrows in **Fig. 1(b)**) are not exactly straight, and instead, are deflected when propagating through the micro-segregation bands within the grain. Inverse pole figure (IPF) map and boundary map (red line: {332}<113>$_\beta$ twin boundary, black line: high angle grain boundary and green colored region: α" phase) of the deformed microstructure are shown in **Fig. 1(c)** and **(d)**, respectively. Most of the plate-like deformation products were identified to be {332}<113>$_\beta$ deformation twins (red lines in **Fig. 1(d)**), except for a few SIM α" (regions with green color in **Fig. 1(d)**) that mainly located at the deflection points where {332}<113>$_\beta$ deformation twins propagated across the Mo-lean bands (indicated by black arrows in **Fig. 1(d)**). This indicates a transition of deformation mode from {332}<113>$_\beta$ twinning to SIM α" transformation (β-twin → α"-martensite) at the chemical interface between the Mo-lean and Mo-rich regions. Although the propagation of deformation twins was generally deflected or even blocked at high angle grain boundaries, to the best of the authors 'knowledge, such a transition of deformation mode in the grain interior was reported for the first time in metastable β titanium alloys. It should also be noted that the propagation of {332}<113>$_\beta$ twins did not change the direction when propagating through the Mo-rich regions.

A more detailed analysis of this transition (β-twin → α"-martensite) was carried out for a single β grain containing Mo-segregation bands (**Fig. 2**). BSE image and grain boundary map (red line: {332}<113>$_\beta$ twin boundary, green colored region: α" phase) of this grain after a plastic strain of 4.5% are shown in **Fig. 2(a)** and **(b)**, respectively. The corresponding Mo mapping obtained by EPMA is shown in **Fig. 2(c)**. A good correlation can be found between the dark bands (**Fig. 2(a)**), α"-martensite plates (**Fig. 2(b)**) and Mo-lean regions with 10~11 wt.% Mo (**Fig. 2(c)**), thereby unambiguously confirming that α"-martensite plates preferentially formed when {332}<113>$_\beta$ twins propagated to the Mo-lean regions (white arrows in **Fig. 2(b)**). In the Mo-rich regions with 11~13 wt.% Mo, on the other hand, the propagation of {332}<113>$_\beta$ twins was straight and no transition was observed. One local region (marked by rectangle in **Fig. 2(a)**) containing such transition is zoomed in, as shown in the BSE image of **Fig. 2(d)**. The angle between the traces of {332}<113>$_\beta$ twin boundary (red dashed line) and the α"-martensite plate (green dashed line) was measured to be ~18 °, which was related to the different habit planes of {332}<113>$_\beta$ twin and α"-martensite ({344}$_\beta$ [28]) with respect to the β matrix. Thin martensitic twin plates with a thickness of 50~150 nm were clearly observed inside the α" plate, which was believed to accommodate the β-α" phase transformation strain [28]. The Mo content profile along the blue line (parallel to the {332}<113>$_\beta$ twin boundary) is shown in **Fig. 2(e)**, in which the occurrence ranges of {332}<113>$_\beta$ twins and α"-martensite were indicated by red and black arrows, respectively. It can be seen that, {332}<113>$_\beta$ twins existed in the Mo content range of 11.2~12.5 wt.%, whereas α"-martensite were detected at the Mo content range of 10.5~11.7 wt.%. At the intermediate Mo range (11.2~11.7 wt.%), both deformation modes coexisted, which indirectly suggests that

α"-martensite could probably nucleates from the interface between {332}<113>$_\beta$ twin tip and the parent β phase, a region generally associated with a high stress concentration [29, 30].

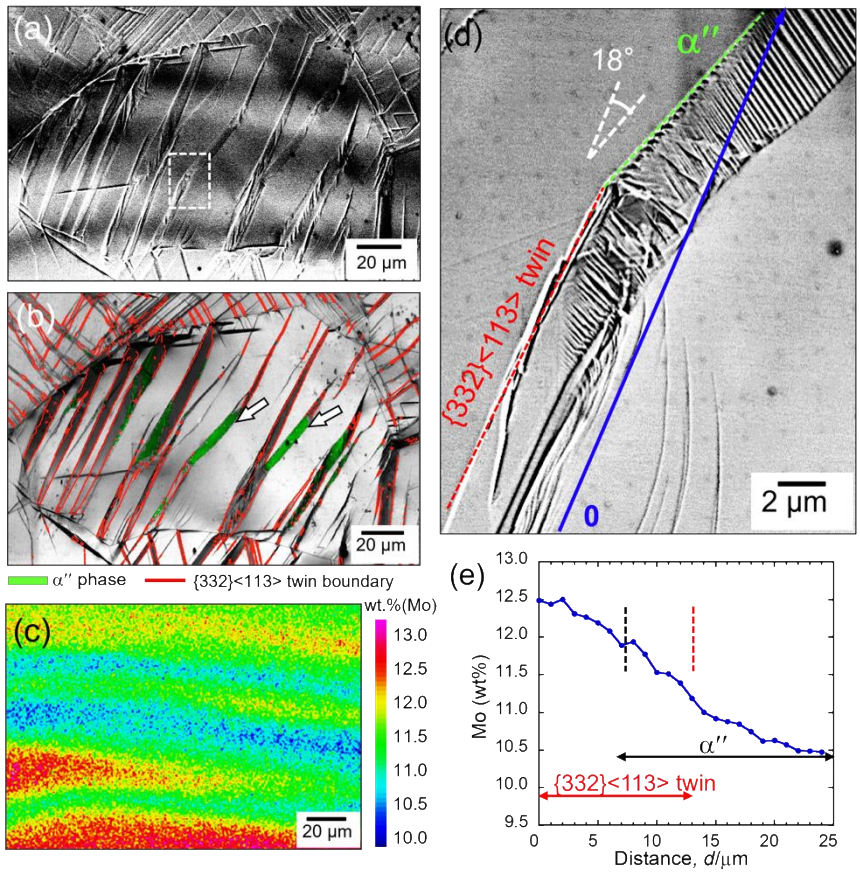

Fig. 2 (a) BSE image of one specific β grain exhibiting the '{332} <113>$_\beta$ twin → α"-martensite transition'. (b) EBSD image quality map of the same area, in which α″ phase and {332} <113>$_\beta$ twin boundaries were shown by green color and red lines. (c) EPMA Mo-mapping of the same area, according to the scale bar on the right. (d) BSE image of the marked region shown in (a). (e) EPMA line analysis of Mo along the blue line in (d), where the ranges of where {332} <113>$_\beta$ twins and α"-martensite occurs are indicated by red and blue arrows, respectively.

It should also be mentioned that some {332} <113>$_\beta$ twins propagated through the Mo-lean bands without any noticeable morphological change, especially for those close to the grain boundary. To explain this phenomenon, the twin propagation behaviors in the same grain as in **Fig. 2(a)** at the early stages (from ε = 0.2% to ε = 2.6%) of plastic deformation were revisited (**Fig. 3**). Boundary maps (with the same illustration method as in **Fig. 2(b)**) of the identical area at interrupted plastic strains are shown in **Fig. 3(b)~(d)**, respectively. Two types of twin propagation was defined, namely type A without β-twin → α"-martensite transition and type B with β-twin → α"-martensite transition. A total of 9 twin propagation events (labelled by numbers) were analyzed, together with the stress and strain at which the event occurred (as summarized in the table of **Fig. 3**). It was revealed by this semi-quantitative analysis that type A twin

propagation (without transition) typically occurred at lower applied stress (σ~515 MPa), whereas type B twin propagation (with transition) was more dominant at relatively higher applied stress (σ~561 MPa).

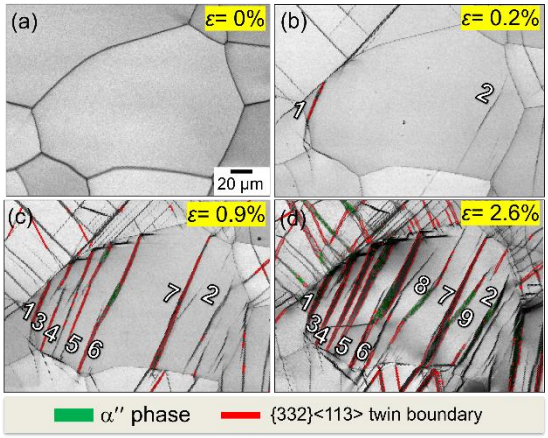

Number of event	Type of twin propagation	σ (MPa)	ε (%)
1	Type-A	515	0.2
2	Type-B		
3	Type-A	546	0.9
4	Type-A		
5	Type-A		
7	Type-A		
6	Type-B		
8	Type-B	561	2.6
9	Type-B		

Fig. 3 (a)-(d) EBSD image quality (IQ) maps showing the evolution of twin propagation events at different interrupted plastic strains in one grain investigated. The summary of two types (type A: without transition, type B: with transition) of twin propagation events at different interrupted strains (ε) and applied stresses (σ) is shown in the table.

These findings indicate that both Mo content and the applied stresses σ play a key role in the propagation of {332}<113>$_\beta$ twins as well as its transition to α"-martensite. Solute atoms can affect the twin propagation behavior by influencing the twinning stress, i.e., the critical stress to propagate twin plates, which scales with the stacking fault energy [31]. However, the Mo content variations in this study (10~13 wt.%) is supposed to have a negligible effect on the twinning stress [9,32]. Therefore, we will rationalize the transition from a thermodynamic standpoint. At the testing temperature T_t, where $M_s<T_t<T_0$ (M_s: martensitic transformation start temperature; T_0: equilibrium temperature), the critical condition for triggering SIM transformation is described as follows [33, 34]:

$$\Delta G_m^{crit} = \Delta G_m^{ch} + \Delta G_m^{\sigma} \quad (1),$$

where ΔG_m^{crit} denotes the molar critical driving force, ΔG_m^{ch} is the chemical free energy difference ($\Delta G_m^{ch} = G_m^{ortho} - G_m^{bcc}$) and ΔG_m^{σ} is the mechanical work caused by the applied stresses σ. The critical driving force (ΔG_m^{crit}) equals the $\Delta G_{m(T=M_s)}^{crit}$ at M_s without external stress. For SIM α" transformation at a given T_t, the value of ΔG_m^{crit} is assumed invariable for β-Ti alloys with different Mo contents [35]. Thus, the required ΔG_m^{σ} is closely related to the ΔG_m^{ch}, *i.e.*, the chemical composition. In the present study, the chemical driving force ΔG_m^{ch} between β and α"-martensite at ambient temperature (298.15 K) is calculated using the TiGen model proposed by Yan and Olson [36]. This model provides thermodynamic data to describe the

kinetic of $\beta \rightarrow \alpha$" martensitic transformation for some binary and ternary Ti alloys. Based on the data, ΔG_m^{ch} was calculated.

In the calculation, the effect of orthorhombic distortion on thermodynamics was neglected and the crystal structure of α"-martensite was assumed to be the same with equilibrium hcp structure. The details of the calculation method are described in Ref. [36]. The results are shown in **Fig. 4**. It is seen that ΔG_m^{ch} decreases linearly with increasing Mo content. For instance, the difference between ΔG_m^{ch} for 10 wt.% Mo and 13 wt.% is estimated as -774.5 J/mol, which is quite comparable [36]. The required mechanical work ΔG_m^{σ} to trigger SIM α" transformation is hence greatly reduced at the Mo-lean regions. This effect agrees with the present result, where the SIM α" plates mainly occur in Mo-lean micro-segregation bands, **Fig.1 (b)** and **Fig. 2(a)**.

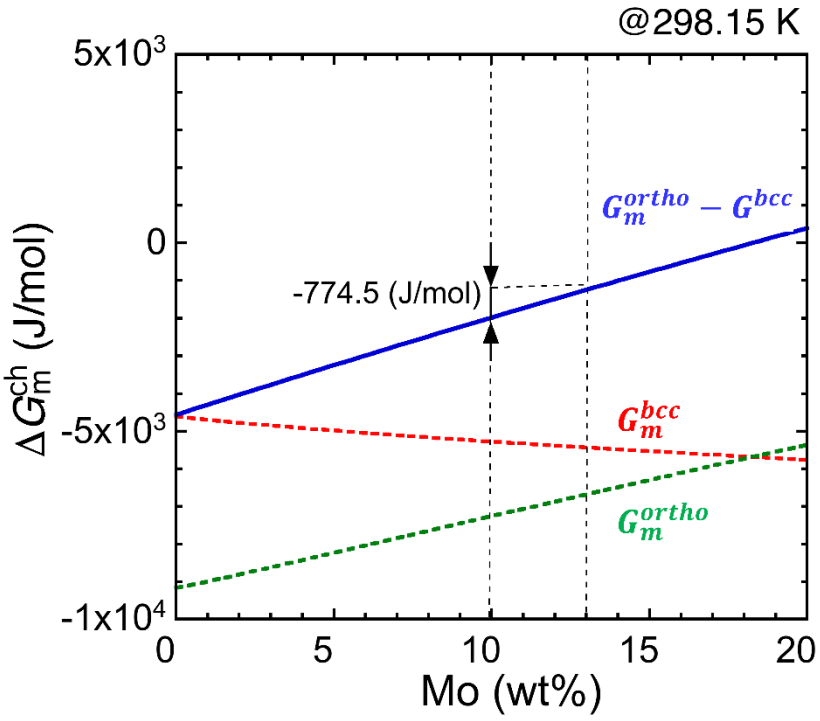

Fig. 4 Calculated molar chemical free energy of ΔG_m^{ch}(=$G_m^{ortho} - G_m^{bcc}$) together with G_m^{ortho} and G_m^{bcc} as a function of Mo content at ambient temperature (298.15K).

Moreover, the mechanical work term ΔG_m^{σ} is proportional to the applied stress, according to Patch and Cohen's model [33] of $\Delta G_m^{\sigma} = \tau_s\gamma_0 + \sigma_n\varepsilon_0 = \frac{1}{2}\sigma\gamma_0 \sin 2\theta + \frac{1}{2}\sigma\varepsilon_0(1 + \cos 2\theta)$,where $\tau_s\gamma_0$ and $\sigma_n\varepsilon_0$ represent the work done by the shear and normal stresses, respectively, γ_0 is the associated shear strain, ε_0 is the dilatational strain, and θ is the angle between the stress axis and the normal to the habit plane. In this

context, a higher applied stress can increase the driving force for phase transformation, thus explaining a more frequent occurrence of type B β-twin → α"-martensite transition at larger stress level, **Fig.3 (c)** and **Fig. 3(d)**.

From the above thermodynamic analysis, we can now explain our observations (**Fig. 5**). In the analyzed grain with Mo gradient (10 - 13 wt.%), the required mechanical work ΔG_m^σ to trigger the martensitic transformation varied during the twin propagation (**Fig. 5(a)**). At relatively higher applied stress, the transition of deformation modes (β-twin → α"-martensite) occurred during the twin propagation where ΔG_m^σ is satisfied for specific Mo content (~12 wt.% in Fig.2 (e)) (**Fig. 5(b)-(c)**). Similarly, SIM α" transformation stopped at the Mo interface in the Mo-rich band where ΔG_m^σ cannot be reached, followed by α"-martensite → β-twin deformation (**Fig. 5(d)**). It can be revealed that the transitions of deformation modes (β-twin → α"-martensite and further α"-martensite → β-twin) depending on the Mo content, namely, β phase stability.

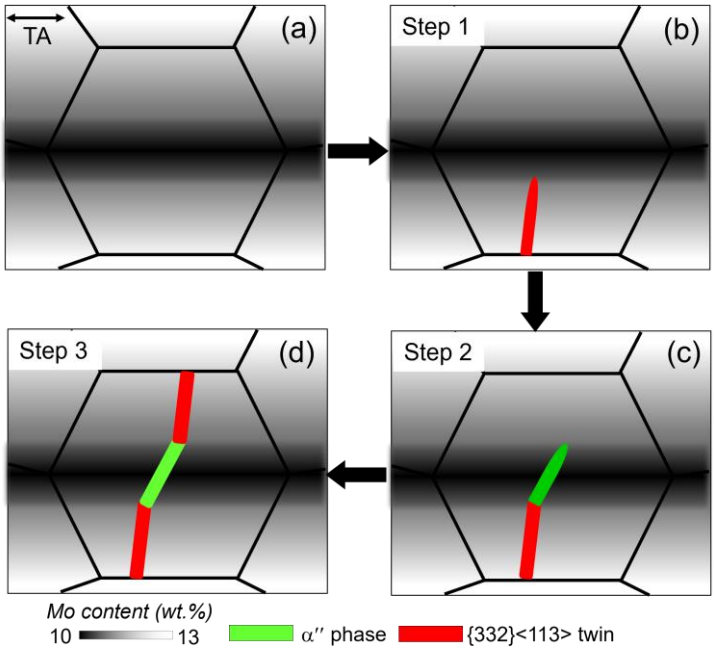

Fig. 5 Schematically illustration of the deformation behaviors of a Ti-12Mo alloy with chemically heterogeneous microstructure. The gradient from black to white indicates increment of Mo content from 10 to 13 wt.%. The green and red color indicate α″ and {332}<113> twin plates, respectively.

In summary, the propagation behavior of {332}<113>$_\beta$ twins in a chemically heterogeneous Ti-12.0 Mo alloy (with Mo content ranging from 10 to 13 wt.%) was investigated. The transition from {332}<113>$_\beta$ twinning to α" martensitic transformation occurred along the twin propagation path when the twins

propagated from the Mo-rich (11.2 ~12.5 wt.%) to Mo-lean (10.5~11.7 wt.%) region. This transition was preferentially found at relatively larger stress, along with a deflection angle of ~18°. By thermodynamic analysis, it is found that the stability of β phase, i.e. the local Mo content and applied stress governed the activation of α" martensitic transformation as well as the propagation of {332}<113>$_\beta$ twins.

Acknowledgments

This work was partly supported by JSPS Grant-in-Aid for Scientific Research (C) (KAKENHI) Grant Number JP26420733.

References:

[1] S. Hanada, T. Yoshio, O. Izumi, Effect of plastic deformation modes on tensile properties of beta titanium alloys, Trans. Japan Inst. Met. 27 (1986) 496–503.

[2] R.P. Kolli, W.J. Joost, S. Ankem, Phase stability and stress-induced transformations in beta titanium alloys, JOM 76 (2015) 1273–1280.

[3] M. Marteleur, F. Sun, T. Gloriant, P. Vermaut, P.J. Jacques, F. Prima, On the design of new β metastable titanium alloys with improved work hardening rate thanks to simultaneous TRIP and TWIP effects, Scr. Mater. 66 (2012) 749–752.

[4] B.N. Qian, L. Lilensten, J.Y. Zhang, M. Yang, F. Sun, P. Vermaut, F. Prima, On the transformation pathways in TRIP/TWIP Ti-12Mo alloy, Mater. Sci. Eng. A 822 (2021) 141672.

[5] B.N. Qian, S.A. Mantri, S. Dasari, J.Y. Zhang, L. Lilensten, F. Sun, P. Vermaut, R. Banerjee, F. Prima, Mechanisms underlying enhanced strength-ductility combinations in TRIP/TWIP Ti-12Mo alloy engineered via isothermal omega precipitation, Acta Mater. 245 (2023) 118619.

[6] G. Welsch, R. Boyer, E.W. Collings, in: G. Welsch, R. Boyer, E.W. Collings (Eds.), Mater. Prop. Handb. Titan. Alloy., ASM International, (1999) 5–11.

[7] T.W. Duerig, J. Albrecht, D. Richter, P. Fischer, Formation and reversion of stress induced martensite in Ti-10V-2Fe-3Al, Acta Metall. 30 (1982) 2161–2172.

[8] L.C. Zhang, T. Zhou, M. Aindow, S.P. Alpay, M.J. Blackburn, Nucleation of stress-induced martensites in a Ti/Mo-based alloy, J. Mater. Sci. 40 (2005) 2833–2836.

[9] X.H. Min, S. Emura, T. Nishimura, K. Tsuchiya, K. Tsuzaki, Microstructure, tensile deformation mode and crevice corrosion resistance in Ti-10Mo-xFe alloys, Mater. Sci. Eng. A 527 (2010) 5499–5506.

[10] K. Cho, R. Morioka, S. Harjo, T. Kawasaki, H. Yasuda, Study on formation mechanism of {332}<113> deformation twinning in metastable β-type Ti alloy focusing on stress-induced ”αmartensite phase, Scripta Mater. 177 (2020) 106-111.

[11] P. Kwasniak, F. Sun, S. Mantri, R. Banerjee, F. Prima, Polymorphic nature of {332}<113> twinning mode in BCC alloys, Mater. Res. Lett. 10 (2022) 334-342.

[12] S. Hanada, O. Izumi, Correlation of tensile properties, deformation modes, and phase stability in commercial β-phase titanium alloys, Metall. Trans. A 18 (1987) 265–271.

[13] X.H. Min, K. Tsuzaki, S. Emura, K. Tsuchiya, Enhancement of uniform elongation in high stength Ti-Mo based alloys by combination of deformation modes, Mater. Sci. Eng. A 528 (2011) 4569–4578.

[14] F. Sun, J.Y. Zhang, M. Marteleur, T. Gloriant, P. Vermaut, D. Laillé, P. Castany, C. Curfs, P.J. Jacques, F. Prima, Investigation of early stage deformation mechanisms in a metastable β titanium alloy combined with twinning-induced plasticity and transformation-induced plasticity effects Acta Mater. 61 (2013) 6406–6417.

[15] M.J. Blackburn, J.A. Feeney, Stress-induced transformations in Ti-Mo alloys, J. Inst. Met. 99 (1971) 132–134.

[16] A.. Crocker, Twinned martensite, Acta Metall. 10 (1962) 113–122.

[17] H. Tobe, H.Y. Kim, T. Inamura, H. Hosoda, S. Miyazaki, Origin of {332} twinning in metastable β-Ti alloy, Acta Mater. 64 (2014) 345–355.

[18] V.S. Litvinov, G.M. Rusakov, Twinning on the {332}<113> system in unstable β-titanium alloy, Phys. Met. Metallogr. 90 (2000).

[19] M.J. Lai, C.C. Tasan, D. Raabe, On the mechanism of {332} twinning in metastable β titanium alloy, Acta Mater. 111 (2016) 173–186.

[20] J.W. Christian, S. Mahajant, Deformation twinning, Prog. Mater. Sci. 39 (1995) 1–157.

[21] C. Hutchinson, A novel experimental approach to identifying kinetic transitions in solid state phase transformations, Scr. Mater. 50 (2004) 285–290.

[22] M. Gouné, F. Danoix, J. Ågren, Y. Bréchet, C.R. Hutchinson, M. Militzer, G. Purdy, S. van der Zwaag, H. Zurob, Overview of the current issues in austenite to ferrite transformation and the role of migrating interfaces therein for low alloyed steels, Mater. Sci. Eng. R Reports 92 (2015) 1–38.

[23] F. De Geuser, M.J. Styles, C.R. Hutchinson, A. Deschamps, High-throughput in-situ characterization and modeling of precipitation kinetics in compositionally graded alloys, Acta Mater. 101 (2015) 1–9.

[24] I. Gutierrez-Urrutia, C.-L. Li, S. Emura, X. Min, K. Tsuchiya, Study of {332}<113> twinning in a multilayered Ti-10Mo-xFe (x = 1-3) alloy by ECCI and EBSD, Sci. Technol. Adv. Mater. 17 (2016) 220–228.

[25] X. Min, S. Emura, F. Meng, G. Mi, K. Tsuchiya, Mechanical twinning and dislocation slip multilayered deformation microstructures in β-type Ti-Mo based alloy, Scr. Mater. 102 (2015) 79–82.

[26] X. Ji, Y. Chong, S. Emura, K. Tsuchiya, Heterogeneous distribution of isothermal ω precipitates prevents brittle fracture in aged β-Ti alloys, Scripta Mater. 241 (2024) 115879.

[26] S. Emura, X.H. Min, S. Ii, K. Tsuchiya, Effect of swirly segregation of Mo on omega phase precipitation behavior and tensile property of Ti-12Mo alloy, Key Eng. Mater. 551 (2013) 180–185.

[27] T. Inamura, J.I. Kim, H.Y. Kim, H. Hosoda, K. Wakashima, S. Miyazaki, Composition dependent crystallography of α"-martensite in Ti-Nb-based β-titanium alloy, Philos. Mag. 87 (2007) 3325–3350.

[28] Z. Jin, T.R. Bieler, Back-stress distribution along a thin twin layer in TiAl, Mater. Sci. Eng. A 192-193 (1995) 729–732.

[29] R.M. Wood, Martensitic alpha and omega phases as deformation products in a titanium-15% molybdenum alloy, Acta Metall. 11 (1963) 907–914.

[30] M.A. Meyers, O. Vöhringer, V.A. Lubarda, The onset of twinning in metals: a constitutive description, Acta Mater. 49 (2001) 4025–4039.

[31] Y. Takemoto, I. Shimizu, A. Sakakibara, T. Senuma, Martensitic transformation induced at low and high temperatures on Ti-15V-7Al alloy, J. Japan Inst. Met. 70 (2006) 110–113.

[32] J.R. Patel, M. Cohen, Criterion for the action of applied stress in the martensitic transformation, Acta Metall. 1 (1953) 531–538.

[33] I. Tamura, Deformation-induced martensitic transformation and transformation-induced plasticity in steel, Met. Sci. 16 (1982) 245–253.

[34] T. Grosdidier, Y. Combres, E. Gautier, M.-J. Philippe, Effect of microstructure variations on the formation of deformation-induced martensite and associated tensile properties in a β metastable Ti alloy, Metall. Mater. Trans. A 31 (2000) 1095–1106.

[35] J.Y. Yan, G.B. Olson, Computational thermodynamics and kinetics of displacive transformations in titanium-based alloy, J. Alloys Compd. 673 (2016) 441–454.